Transient effects and reconstruction of the energy spectra in the time evolution of transmitted Gaussian wave packets

2010 J. Phys. A: Math. Theor. 43 185301

(http://iopscience.iop.org/1751-8121/43/18/185301)

IOP PUBLISHING JOURNAL OF PHYSICS A: MATHEMATICAL AND THEORETICAL

J. Phys. A: Math. Theor. **43** (2010) 185301 (17pp) doi:10.1088/1751-8113/43/18/185301

Transient effects and reconstruction of the energy spectra in the time evolution of transmitted Gaussian wave packets

Sergio Cordero and Gastón García-Calderón[1]

Instituto de Física, Universidad Nacional Autónoma de México, Apartado postal 20–364, México 01000, Distrito Federal, Mexico

E-mail: gaston@fisica.unam.mx

Received 9 November 2009, in final form 12 March 2010
Published 15 April 2010
Online at stacks.iop.org/JPhysA/43/185301

Abstract

We derive an analytical solution to the time-dependent Schrödinger equation for the transmission of a Gaussian wave packet through an arbitrary potential of finite range. We consider the situation where the initial Gaussian wave packet is sufficiently broad in momentum space to include the full resonance structure of the system in the dynamical description. We find that the transmitted wave packet may be written as the free evolving Gaussian wave packet solution times a transient term. We demonstrate that both at very large distances and very long times the transient term tends to the transmission amplitude of the system and hence the time-evolving solution reproduces the resonance spectra of the system. We also prove that at a fixed distance and very long times the analytical solution is $t^{-3/2}$ which extends previous analysis on this issue to arbitrary finite-range potentials. Our results are exemplified for a multibarrier system.

PACS numbers: 03.65.Ca, 03.65.Nk, 03.65.Db, 73.40.Gk

(Some figures in this article are in colour only in the electronic version)

1. Introduction

The transmission of wave packets through one-dimensional potentials is a model that has been of great relevance both from a pedagogical point of view, as discussed in many quantum mechanics textbooks, and in research, particularly since the advent of artificial semiconductor quantum structures [1, 2]. There are studies on the dynamics of tunneling [3–9] or work on controversial issues, such as the tunneling time problem [10–13], and on related topics, such as the Hartman effect [14, 15] or the delay time [16–18]. Most time-dependent numerical

[1] Author to whom any correspondence should be addressed.

studies consider Gaussian wave packets as initial states [2, 5, 19, 20], though in some recent work, the formation of a quasistationary state in the scattering of wave packets on finite one-dimensional periodic structures also involves some analytical considerations [21, 22]. Analytical approaches have been mainly concerned with cutoff quasi-monochromatic initial states in a quantum shutter setup [3, 18, 23–25]. In recent work, however, analytical solutions to the time-dependent wavefunction have been discussed using initial Gaussian wave packets for square barriers [15, 26], delta potentials [6, 26] and resonant tunneling systems near a single resonance [9].

We obtain an analytical solution to the time-dependent Schrödinger equation for transmission of an initial Gaussian wave packet through an arbitrary potential of finite range. We refer to the physically relevant case where the initial Gaussian wave packet is sufficiently far from the interaction region so that the corresponding tail near that region is very small and hence may be neglected. Since the infinite limit of a very broad cutoff Gaussian wave packet in configuration space, i.e. that leading to a cutoff plane wave, has been discussed analytically elsewhere [3], we focus the discussion here to cases where the initial cutoff Gaussian wave packet is sufficiently broad in momentum space so that all the resonances of the quantum system are included in the dynamical description. We demonstrate that the profile of the transmitted wave packet exhibits a transient behavior which at very large distances and long times may be expressed as the free evolving wave packet modulated by the transmission amplitude of the system. To the best of our knowledge, this is a novel and an interesting result. We also analyze the transmitted solution at a fixed distance away from the potential at very long times, and find that it behaves as $t^{-3/2}$. Our result generalizes previous analysis, involving specific potential models and numerical calculations [27], to arbitrary potentials of finite range. Other asymptotic inverse power-law behaviors have also been investigated by considering distinct momentum characteristics of the initial sate [28]. The long-time, post-exponential, behavior is also a subject of current interest in decay problems [29, 30] and in studies involving a large class of linear differential equations [31].

The present work may also be seen in the framework of studies on transient phenomena in quantum systems [32].

The paper is organized as follows. In section 2, the integral expression for the transmitted cutoff Gaussian wave packet is derived. Section 3 discusses the resonance expansion of the transmission amplitude and for the analytical solution for the transmitted wave packet. Also some relevant limits are considered. Section 4 discusses an example in detail, specifically a quadruple barrier resonant tunneling system. Section 5 gives some remarks concerning the tunneling time problem. Section 6 provides the concluding remarks and, finally, the appendices discuss, respectively, the analysis of the effect of the cutoff in the solution, and a general method to calculate the complex poles of the transmission amplitude.

2. Transmitted time-dependent solution for a cutoff Gaussian pulse

Let us consider the time evolution of an initial state $\psi(x,0)$ of a particle of energy $E_0 = \hbar^2 k_0^2/2m$, approaching from $x < 0$ toward a potential $V(x)$ that extends along the interval $0 < x < L$. The time-dependent solution along the transmitted region $x \geqslant L$ reads [25, 33]

$$\psi(x,t) = \frac{1}{\sqrt{2\pi}} \int_{-\infty}^{\infty} \mathrm{d}k\, \phi_0(k) \mathbf{t}(k)\, \mathrm{e}^{\mathrm{i}kx - \mathrm{i}\hbar k^2 t/2m}, \tag{1}$$

where $\mathbf{t}(k)$ is the transmission amplitude of the problem and $\phi_0(k)$ is the Fourier transform of the initial function $\psi(x,0)$. We consider as initial state the cutoff Gaussian wave packet

$$\psi(x,0) = \begin{cases} A_0 \mathrm{e}^{-(x-x_\mathrm{c})^2/4\sigma^2} \mathrm{e}^{\mathrm{i}k_0 x}, & x < 0 \\ 0, & x > 0, \end{cases} \tag{2}$$

where A_0 is the normalization constant, and x_c, σ and k_0 are, respectively, the center, the effective width and the wavenumber corresponding to the incident energy E_0 of the wave packet. The Fourier transform of the initial Gaussian cutoff wave packet is given by [26]

$$\phi_0(k) = A_0\, \omega(\mathrm{i}z), \tag{3}$$

where

$$A_0 = \frac{1}{(2\pi)^{1/4}} \left(\frac{\sigma}{\omega(\mathrm{i}z_0)} \right)^{1/2} \tag{4}$$

with z and z_0 given respectively by

$$z = \frac{x_\mathrm{c}}{2\sigma} - \mathrm{i}(k - k_0)\sigma, \tag{5}$$

and

$$z_0 = \frac{x_\mathrm{c}}{\sqrt{2}\,\sigma}, \tag{6}$$

and $\omega(\mathrm{i}z)$ is the Faddeyeva function [34, 35].

Let us place the initial wave packet along the region $x_\mathrm{c} < 0$. As pointed out above, here we shall be concerned with the physically relevant situation where the tail of the initial Gaussian wave packet is very small near the interaction region. It is then convenient to consider the symmetry relationship of the Faddeyeva function [34, 35]

$$\omega(\mathrm{i}z) = 2\,\mathrm{e}^{z^2} - \omega(-\mathrm{i}z) \tag{7}$$

and follow an argument given by Villavicencio *et al* for the free and δ potential cases [26]. These authors obtain that provided

$$\left| \frac{x_\mathrm{c}}{2\sigma} \right| \gg 1, \qquad x_\mathrm{c} < 0, \tag{8}$$

one may approximate $\omega(\mathrm{i}z)$ as

$$\omega(\mathrm{i}z) \simeq 2\,\mathrm{e}^{z^2}. \tag{9}$$

In appendix A we show that the above approximation holds also for the general case of finite-range potentials. Note that the above considerations apply also for $\omega(\mathrm{i}z_0)$ so $\omega(\mathrm{i}z_0) \approx 2\exp\left(z_0^2\right)$. As a consequence the normalization constant, given by (4), may be written as

$$A_0 \approx \frac{1}{(2\pi)^{1/4}} \left(\frac{\sigma}{2} \right)^{1/2} \mathrm{e}^{-x_\mathrm{c}^2/4\sigma^2}. \tag{10}$$

Substitution of (9) into (3) and the resulting term into (1) allows us to write the time-dependent solution as

$$\psi^\mathrm{a}(x,t) = D\,\mathrm{e}^{\mathrm{i}k_0 x - \mathrm{i}\hbar k_0^2 t/2m} \frac{\mathrm{i}}{2\pi} \int_{-\infty}^{\infty} \mathrm{d}q\; \mathbf{t}(q + k_0)\, \mathrm{e}^{\mathrm{i}qx' - \mathrm{i}\hbar q^2 t'/2m}, \tag{11}$$

where the index a is to recall that the solution holds provided (8) is satisfied, and we have

$$D = -2\mathrm{i}(2\pi)^{1/4}\sqrt{\sigma/2}, \tag{12}$$

$$q = k - k_0 \tag{13}$$

and

$$x' = x - x_\mathrm{c} - \frac{\hbar k_0}{m} t, \qquad t' = t - \mathrm{i}\tau, \tag{14}$$

with τ,

$$\tau = \frac{2m\sigma^2}{\hbar}. \tag{15}$$

From equation (11) it follows immediately that the free evolving solution, i.e. $\mathbf{t}(k) = 1$, may be written as

$$\psi_{\mathrm{f}}^{\mathrm{a}}(x,t) = \frac{1}{(2\pi)^{1/4}}\frac{1}{\sigma^{1/2}}\frac{\mathrm{e}^{\mathrm{i}(k_0 x - \hbar k_0^2 t/2m)}\,\mathrm{e}^{\mathrm{i}mx'^2/2\hbar t'}}{\sqrt{1+\mathrm{i}t/\tau}}, \tag{16}$$

that is identical to the exact analytical expression for an extended initial Gaussian wave packet [26].

3. Analytical solution for the transmitted Gaussian pulse

The expression for the transmitted time-dependent solution given by equation (11) is amenable for numerical evaluation by well-known procedures. Here we derive an analytical solution to equation (11). Our approach exploits the analytical properties of the outgoing Green's function on the complex k plane. In order to accomplish this, it is convenient to write the transmission amplitude in terms of the outgoing Green's function to the problem. This may be obtained immediately by considering the continuum solutions $\psi(k,x)$ to the Schrödinger equation of the problem [36]

$$\frac{\mathrm{d}^2}{\mathrm{d}x^2}\psi(k,x) + [k^2 - U(x)]\psi(k,x) = 0, \tag{17}$$

where $U(x) = 2mV(x)/\hbar^2$. Outside the interaction range, say for incidence from the left, the corresponding solutions of a particle of energy $E = \hbar k^2/2m$ may be written respectively as $\psi(k,x) = \exp(\mathrm{i}kx) + \mathbf{r}(k)\exp(-\mathrm{i}kx)$, $x \leqslant 0$, and $\psi(k,x) = \mathbf{t}(k)\exp(\mathrm{i}kx)$, $x \geqslant L$, where $\mathbf{r}(k)$ stands for the reflection amplitude. Next, we consider Green's theorem between the equation for $\psi(k,x)$ and that for the outgoing Green's function to the problem $G^+(x,x';k)$,

$$\frac{\mathrm{d}^2}{\mathrm{d}x^2}G^+(x,x';k) + [k^2 - U(x)]G^+(x,x';k) = \delta(x-x'), \tag{18}$$

which obeys outgoing boundary conditions, i.e. $G^{+\prime}(0,x';k) = -\mathrm{i}kG^+(0,x';k)$ and $G^{+\prime}(L,x';k) = \mathrm{i}kG^+(L,x';k)$, the prime meaning derivative with respect to x evaluated respectively, in each expression, at $x = 0$ and $x = L$. The above leads to the following relationship for the continuum wavefunction along the internal interaction region:

$$\psi(k,x) = 2\mathrm{i}kG^+(0,x;k), \qquad 0 \leqslant x \leqslant L. \tag{19}$$

Considering the solution of the wavefunction at $x = L$ allows us to write the transmission amplitude as

$$\mathbf{t}(k) = 2\mathrm{i}kG^+(0,L;k)\,\mathrm{e}^{-\mathrm{i}kL}. \tag{20}$$

It is well known that the function $G^+(x,x';k)$, and consequently the transmission amplitude $\mathbf{t}(k)$, possesses an infinite number of complex poles κ_n, in general simple, distributed on the complex k plane in a well-known manner [37]. Purely positive and negative imaginary poles $\kappa_n \equiv \mathrm{i}\gamma_n$ correspond, respectively, to bound and antibound (virtual) states, whereas complex poles are distributed along the lower half of the k plane. We denote the complex poles on the fourth quadrant by $\kappa_n = \alpha_n - \mathrm{i}\beta_n$. It follows from time-reversal considerations [38] that those on the third quadrant, κ_{-n}, fulfill $\kappa_{-n} = -\kappa_n^*$. The complex poles may be calculated by using iterative techniques as the Newton–Raphson method [39], as discussed in

appendix B. Usually one may obtain a resonance expansion for $\mathbf{t}(k)$ by expanding $G^+(0, L; k)$ in terms of its complex poles and residues [40]. Here we find more convenient to expand instead $G^+(0, L; k)\exp(-\mathrm{i}kL)$. In our case, the resonance expansion of $\mathbf{t}(q + k_0)$ reads

$$\mathbf{t}(q + k_0) = \mathrm{i}(q + k_0) \sum_{n=-\infty}^{\infty} \frac{r_n}{q - \kappa_n'} \mathrm{e}^{-\mathrm{i}\kappa_n L}, \tag{21}$$

where

$$\kappa_n' = \kappa_n - k_0 \tag{22}$$

and the quantities r_n correspond to the residues at the poles of the outgoing Green's function of the problem [3]. It is worth mentioning that the residues may be written as[2]

$$r_n = \frac{u_n(0)u_n(L)}{\kappa_n}. \tag{23}$$

Here the functions $u_n(x)$ satisfy the Schrödinger equation to the problem with complex eigenvalues $E_n = \hbar^2\kappa_n^2/2m = \mathcal{E}_n - \mathrm{i}\Gamma_n/2$ and obey the purely outgoing boundary conditions [3, 41]

$$\left[\frac{\mathrm{d}}{\mathrm{d}x}u_n(x)\right]_{x=0} = -\mathrm{i}\kappa_n u_n(0), \qquad \left[\frac{\mathrm{d}}{\mathrm{d}x}u_n(x)\right]_{x=L} = \mathrm{i}\kappa_n u_n(L), \tag{24}$$

and are normalized according to the condition [3]

$$\int_0^L u_n^2(x)\,\mathrm{d}x + \mathrm{i}\frac{u_n^2(0) + u_n^2(L)}{2\kappa_n} = 1. \tag{25}$$

It is now convenient to express the term $(q + k_0)/(q - \kappa_n')$ appearing in (21) as

$$\frac{q + k_0}{q - \kappa_n'} = 1 + \frac{\kappa_n}{q - \kappa_n'}. \tag{26}$$

Then by the substitution of (21) into (11), using (26), allows us to write $\psi^{\mathrm{a}}(x, t)$ as

$$\psi^{\mathrm{a}}(x, t) = C\psi_{\mathrm{f}}^{\mathrm{a}}(x, t) + \sum_{n=-\infty}^{\infty} \psi_n^{\mathrm{a}}(x, t), \tag{27}$$

where C is a constant that depends only on the potential through the values of the r_n's and κ_n's,

$$C = \mathrm{i} \sum_{n=-\infty}^{\infty} r_n \mathrm{e}^{-\mathrm{i}\kappa_n L}, \tag{28}$$

and $\psi_n^{\mathrm{a}}(x, t)$ reads

$$\psi_n^{\mathrm{a}}(x, t) = \mathrm{i}Dr_n\kappa_n \mathrm{e}^{-\mathrm{i}\kappa_n L} \mathrm{e}^{\mathrm{i}k_0 x - \mathrm{i}\hbar k_0^2 t/2m} M(y_n'), \tag{29}$$

where we recall that D is given by (12), and $M(y_n')$ stands for the Moshinsky function, defined as [3, 23]

$$M(y_n') = \frac{\mathrm{i}}{2\pi} \int_{-\infty}^{\infty} \mathrm{d}k \frac{\mathrm{e}^{\mathrm{i}kx' - \mathrm{i}\hbar k^2 t'/2m}}{k - \kappa_n'}. \tag{30}$$

The Moshinsky function is usually calculated via the Faddeyeva functions for which well-developed computational routines are available [42]. These functions are related by

$$M(y_n') = \tfrac{1}{2}\mathrm{e}^{\mathrm{i}mx'^2/2\hbar t'}\omega(\mathrm{i}y_n'), \tag{31}$$

[2] Note that in deriving (19) and (21) we have absorbed the coefficient $\hbar^2/2m$ into the definition of $G^+(x, x'; k)$; otherwise in the residue r_n given by (23) the factor $2m/\hbar^2$ would appear. These factors would cancel out exactly in writing the expansion given by (21).

with

$$y'_n = \mathrm{e}^{-\mathrm{i}\pi/4}\sqrt{\frac{m}{2\hbar t'}}\left[x' - \frac{\hbar\kappa'_n}{m}t'\right]. \tag{32}$$

It is convenient to substitute (31) into (29) and make use of (16) and (28) to write equation (27) for the time-dependent solution as

$$\psi^{\mathrm{a}}(x,t) = \psi^{\mathrm{a}}_{\mathrm{f}}(x,t)\mathcal{T}(x,t), \tag{33}$$

where $\psi^{\mathrm{a}}_{\mathrm{f}}(x,t)$ is given by (16) and $\mathcal{T}(x,t)$ represents a transient contribution given by

$$\mathcal{T}(x,t) = \mathrm{i}\sum_{n=-\infty}^{\infty} r_n\,\mathrm{e}^{-\mathrm{i}\kappa_n L}[1 - \mathrm{i}\pi^{1/2}\sigma\sqrt{1+\mathrm{i}t/\tau}\,\kappa_n\omega(\mathrm{i}y'_n)]. \tag{34}$$

Equation (33) constitutes the main result of this work. It provides an analytical solution for the time evolution of the transmitted Gaussian wave packet that consists of the free evolving Gaussian pulse times a transient term (34). One should emphasize that the above result holds provided the condition given by equation (8) is satisfied. As a consequence of this condition, the solution $\psi^{\mathrm{a}}(x,t)$ does not vanish exactly as $t \to 0$, since there remains a small value proportional to the tail of the free solution. On the other hand, at asymptotically long times, i.e. $|y'_n| \gg 1$, the leading terms of the asymptotic expansion of the Faddeyeva function $\omega(\mathrm{i}y'_n)$ in (34) behave as [35]

$$\omega(\mathrm{i}y'_n) \approx \begin{cases} \dfrac{1}{\pi^{1/2}}\left(\dfrac{1}{y'_n} - \dfrac{3/2}{y'^3_n}\right), & -\pi/2 < \arg y'_n < \pi/2 \\ \mathrm{e}^{y'^2_n} + \dfrac{1}{\pi^{1/2}}\left(\dfrac{1}{y'_n} - \dfrac{3/2}{y'^3_n}\right), & \pi/2 < \arg y'_n < 3\pi/2. \end{cases} \tag{35}$$

The above result will be useful in the next subsections.

3.1. Long-time behavior of $\psi^{\mathrm{a}}(x,t)$

Let us now analyze equation (33) at asymptotically long times, i.e. much larger than the lifetime τ_0 of the system (characterized by the smallest energy width, i.e., $\tau_0 = \hbar/\Gamma_{\min}$), for a fixed value of the distance $x = x_{\mathrm{d}}$. In such a case, one sees from equation (32) that the argument y'_n of the Faddeyeva functions behaves as

$$y'_n \approx -\mathrm{e}^{-\mathrm{i}\pi/4}\sqrt{\frac{\hbar}{2m}}\kappa_n t^{1/2}, \qquad x = x_{\mathrm{d}}, \qquad t \gg \tau_0, \tag{36}$$

and hence becomes very large as time increases.

One sees, by inspection of equation (35), that for sufficiently long times the full set of resonance poles behaves nonexponentially. Using equations (28) and (35), one may write equation (33) at asymptotically long times as

$$\psi^{\mathrm{a}}(x,t) \approx \psi^{\mathrm{a}}_{\mathrm{f}}(x,t)\sum_{n=-\infty}^{\infty}\mathrm{i}r_n\,\mathrm{e}^{-\mathrm{i}\kappa_n L}\left[1 - \mathrm{e}^{-\mathrm{i}\pi/4}t^{1/2}\frac{1}{\sqrt{2m/\hbar}}\kappa_n\left(\frac{1}{y'_n} - \frac{3/2}{y'^3_n}\right)\right]. \tag{37}$$

By the substitution of equation (36) into equation (37), one sees that the first two terms on the right-hand side of this last equation cancel out exactly and hence, using equation (16) one obtains that $\psi^{\mathrm{a}}(x,t)$ behaves with time as

$$\psi^{\mathrm{a}}(x,t) \sim \frac{1}{t^{3/2}}, \qquad x = x_{\mathrm{d}}, \qquad t \gg \tau_0. \tag{38}$$

It follows from the above expression that the corresponding probability density is $1/t^3$. This long-time behavior of the probability density as an inverse cubic power of time has also been

obtained with other potential models and initial states, including numerical calculations of Gaussian wave packets colliding with square barriers [27]. As pointed out in [27] the above long-time behavior for the probability density is consistent with the definition of the dwell time as a physical meaningful quantity.

3.2. Asymptotic behavior of $\psi^{\mathrm{a}}(x,t)/\psi^{\mathrm{a}}_{\mathrm{f}}(x,t)$

There is another asymptotic limit involving the transmitted wave packet solution given by equation (33). This refers to the limit of $\psi^{\mathrm{a}}(x,t)\big/\psi^{\mathrm{a}}_{\mathrm{f}}(x,t)$ as $x\to\infty$ and $t\to\infty$ with x/t a finite quantity. Previous analysis regarding the time evolution of forerunners for cutoff initial plane waves shows that at very large distances and long times they propagate with velocity $\hbar\alpha_n/m$, satisfying the relationship $x/t=(\hbar\alpha_n/m)$ [43]. This allows us to relate the velocity of the forerunners to the corresponding resonance energy and suggests to consider as an *ansatz* a similar behavior for the k-components of the transmitted Gaussian pulse in those very large limits, namely $x=(\hbar k/m)t$ as $t\to\infty$, such that $\hbar k/m$ is a constant quantity[3]. Hence as x and t attain very large values, one may write the argument y'_n of the Faddeyeva function, given by equation (32), as

$$y'_n\approx \mathrm{e}^{-\mathrm{i}\pi/4}\sqrt{\frac{\hbar}{2m}}[k-\kappa_n]t^{1/2}, \tag{39}$$

where the relationships given by equations (14) and (22) have been used. It follows then, using the leading $1/y'_n$ terms in equation (35), that the term $\sqrt{1+\mathrm{i}t/\tau}\;\omega(\mathrm{i}y'_n)$ appearing in equation (34) tends to $\mathrm{i}/[(\pi^{1/2}\sigma)(k-\kappa_n)]$. Rearranging the remaining terms, equation (33) may be written as

$$\frac{\psi^{\mathrm{a}}(x,t)}{\psi^{\mathrm{a}}_{\mathrm{f}}(x,t)}=\mathbf{t}(k)+\mathrm{O}(1/t), \tag{40}$$

where equation (21) has been used. Equation (40) demonstrates that at very large distances and times, $\psi^{\mathrm{a}}(x,t)\big/\psi^{\mathrm{a}}_{\mathrm{f}}(x,t)$ reproduces the transmission amplitude of the system.

It is worth noting that the result given by equation (40) may also be obtained from equation (11) without performing an analysis involving the poles and residues of the transmission amplitude. By completing squares on the exponential terms of the integrand to equation (11) it follows that this equation may be written as

$$\frac{\psi^{\mathrm{a}}(x,t)}{\psi^{\mathrm{a}}_{\mathrm{f}}(x,t)}=\frac{\sigma}{\sqrt{\pi}}\sqrt{1+\mathrm{i}t/\tau}\int_{-\infty}^{\infty}\mathrm{d}q\;\mathbf{t}(q+k_0)\,\mathrm{e}^{-\mathrm{i}\hbar t'(q-mx'/\hbar t')^2/2m}. \tag{41}$$

For very long times and large distances the above equation may be written as

$$\frac{\psi^{\mathrm{a}}(x,t)}{\psi^{\mathrm{a}}_{\mathrm{f}}(x,t)}\approx\sqrt{\frac{\mathrm{i}\hbar t}{2m\pi}}\int_{-\infty}^{\infty}\mathrm{d}q\;\mathbf{t}(q+k_0)\,\mathrm{e}^{-\mathrm{i}\hbar t(q-(k-k_0))^2/2m}, \tag{42}$$

where we have used that $t'\to t$ and $mx'/\hbar t\to(k-k_0)$. For very long times the integral term to the above equation may be evaluated by the steepest descent method [44]. The corresponding saddle point occurs at $q=k-k_0$ and the Taylor expansion of $\mathbf{t}(q+k_0)$ reads $\mathbf{t}(q+k_0)\approx\mathbf{t}(k)+(q-k+k_0)\dot{\mathbf{t}}(k)+\cdots$, where the dot means derivative with respect to q evaluated at $q=k-k_0$. Hence, it follows that the leading contribution of the integral term in (42) is proportional to $\mathbf{t}(k)$ and as a consequence one sees that equation (42) becomes identical to equation (40).

[3] This assertion is corroborated by the numerical calculations discussed in subsection 4.3.

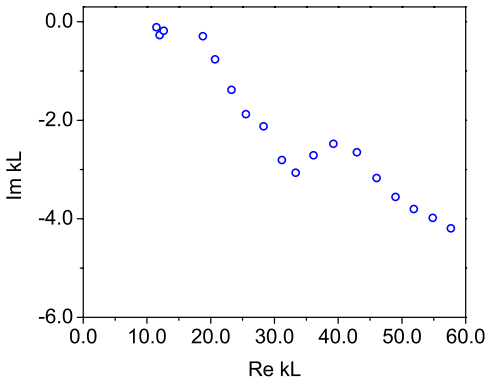

Figure 1. Distribution of the first few poles of the outgoing Green's function on the fourth quadrant of the kL plane for a quadruple barrier resonant tunneling system (QB) (empty circles), with parameters as given in the text.

4. Example and discussion

In order to exemplify our findings, we consider a tunneling system involving typical parameters of semiconductor $Al_xGa_{1-x}As$ materials [1], namely a quadruple-barrier resonant tunneling structure (QB). We choose the following parameters for the system: external barrier widths $b_1 = b_4 = 3.0$ nm, internal barrier widths $b_2 = b_3 = 5.0$ nm, well widths $w_1 = w_2 = w_3 = 3.0$ nm, barrier heights $V = 0.23$ eV and the effective electron mass $m = 0.067\, m_e$, where m_e is the electron mass.

For a given potential profile, the parameters of the system determine the values of the complex poles $\{\kappa_n\}$ which are the relevant ingredients to calculate the resonance states $u_n(x)$ and hence the residues r_n appearing in both equation (21) for the transmission amplitude and equation (33) for the transmitted time-dependent solution. There are a number of procedures to calculate the complex poles. For the sake of completeness, however, we present in appendix B, a convenient procedure to calculate the necessary number of complex poles that relies on the Newton–Raphson iteration method [39]. Once the set of complex poles is obtained, the corresponding set of resonance states $\{u_n(x)\}$ may be obtained using the transfer matrix method [1] with the outgoing boundary conditions given by equation (24).

It is of interest to stress that a given potential profile provides a unique set of resonance poles $\{\kappa_n\}$ and residues $\{r_n\}$ that are calculated only once to evaluate equation (33). This implies that calculations are much less time demanding than calculations involving numerical integration of the solution given by equation (1), where one has to perform an integration over k at each instant of time, particularly if one is interested, as in the present work, to evaluate the above solution at very long times and distances.

4.1. Complex poles and transmission coefficient

Figure 1 exhibits the distribution of the first complex poles for the QB (empty circles) system on the complex kL plane. In this example $L = 25.0$ nm.

Figure 2 shows a plot of the transmission coefficient $T(E) = |\mathbf{t}(E)|^2$ as a function of the energy E in units of the barrier height V. This figure presents a comparison between an exact numerical calculation, using the transfer matrix method (full line), and that obtained using the resonance expansion given by equation (21) (dotted line). One observes that both

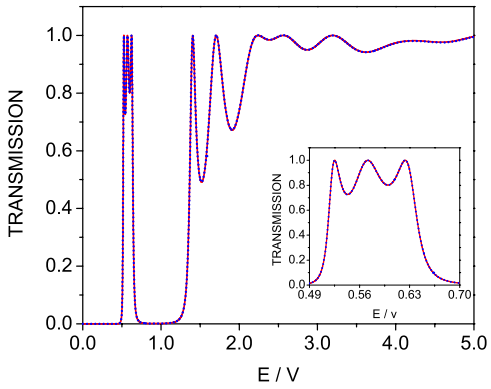

Figure 2. Comparison of the exact numerical calculation of the transmission coefficient (full line) as a function of the energy E in units of the potential height V, with the transmission coefficient obtained from the analytical formula given by (equation (21)) (dotted line) for the QB system. The inset shows the first resonance miniband of the system.

calculations are indistinguishable from each other provided the appropriate number of poles in the resonance expansion is considered, as discussed in appendix B and indicated in the caption to figure B1(a).

Let us comment briefly on some features of figure 2 for the QB system. One sees that it exhibits a triplet of overlapping resonances along the tunneling region, as displayed enlarged in the inset. The corresponding resonance energies are, respectively, $\mathcal{E}_1 = 0.1199$ eV, $\mathcal{E}_2 = 0.1309$ eV and $\mathcal{E}_3 = 0.1450$ eV and the corresponding widths, $\Gamma_1 = 4.6270$ meV, $\Gamma_2 = 11.9652$ meV and $\Gamma_3 = 8.4472$ meV. The QB system exhibits transmission resonances above the barrier height as the energy increases. Note that the triplet of overlapping resonances corresponds to the first triplet of resonance poles exhibited in figure 1 (empty circles). One should mention that the triplet of resonance poles suffices to reproduce the transmission coefficient around the corresponding energy range [40].

4.2. Time evolution of the transmitted probability density

Let us now investigate the time evolution of the transmitted probability density $|\psi^{\mathrm{a}}(x,t)|^2$ using equation (33) as time evolves, for different values of $x = x_{\mathrm{d}}$. We find convenient to plot the dimensionless quantity $\rho(x,t) = \sigma|\psi^{\mathrm{a}}(x,t)|^2$ in units of t/τ, where τ stands for the longest lifetime of the system, i.e. $\tau \equiv \hbar/\Gamma_{\mathrm{min}}$, with Γ_{min} the smallest energy width.

The parameters of the initial cutoff Gaussian wave packet, defined by equation (2), are

$$x_{\mathrm{c}} = -5.0\,\mathrm{nm}, \qquad \sigma = 0.5\,\mathrm{nm}. \tag{43}$$

These values give $|x_{\mathrm{c}}|/(2\sigma) = 5.0$, which implies that the condition given by equation (8) is satisfied, and hence the applicability of equation (33), to calculate the time evolution of the transmitted probability density. Note that $\sigma < L$ for the considered system, i.e. $L_{\mathrm{QB}} = 25.0$ nm. Also, we chose $E_0 = \mathcal{E}_2$ for the QB system. The value of the natural time scale is $\tau_{\mathrm{QB}} = 0.14$ ps.

Figure 3 exhibits the time evolution of the transmitted probability density for the QB system. Figures 3(a)–(c) refer, respectively, to short, $x_{\mathrm{d}} = 2L$, medium, $x_{\mathrm{d}} = 200L$, and large, $x_{\mathrm{d}} = 2 \times 10^5 L$, distances. At short distances, $x_{\mathrm{d}} = 2L$, it is worthwhile to note the presence of Rabi oscillations in a similar fashion as occur in the decay of multibarrier systems [29]. These oscillations represent transitions among the closely lying resonance levels of the

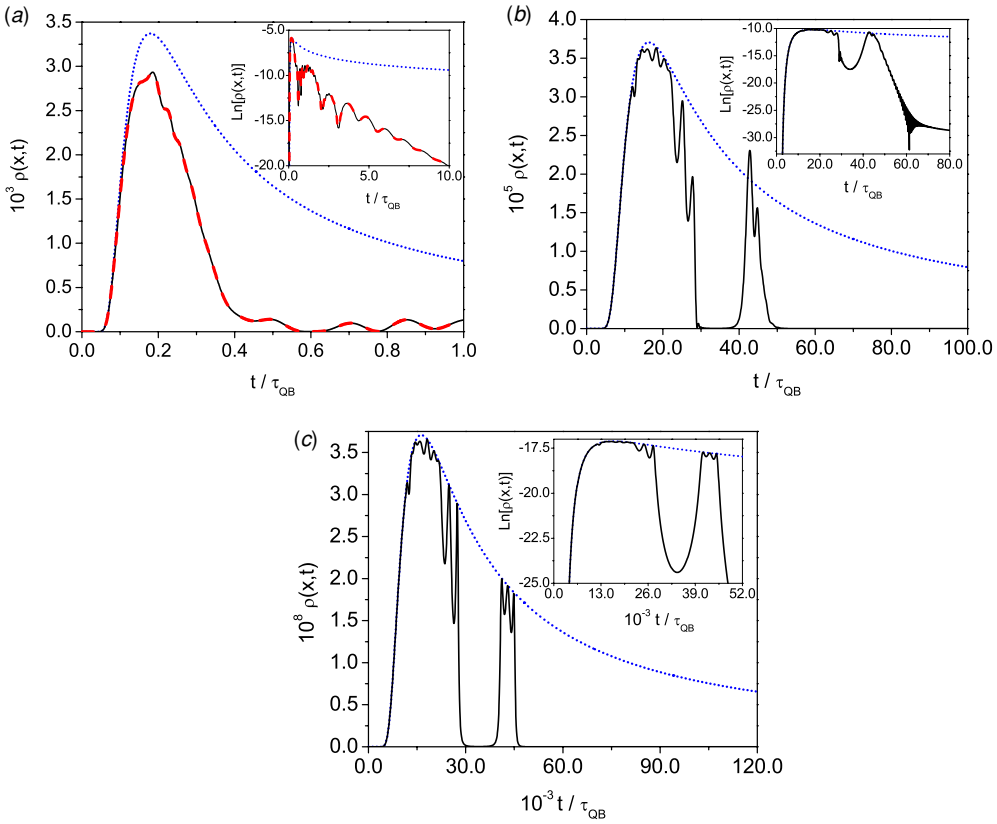

Figure 3. Probability density as a function of the time, in units of the lifetime $\tau_{QB} = \hbar/\Gamma_1$, for the QB system (full line). The energy of the initial Gaussian state is equal to the resonance energy $E_0 = \mathcal{E}_2$. As a comparison the free Gaussian wave packet is plotted (dotted line). The calculation is performed at (*a*) $x_d = 2L$ short, (*b*) $x_d = 200L$ medium and (*c*) $x_d = 2 \times 10^5 L$ long distances, where L is the length of the QB system. The inset shows similar calculations in the semi-ln scale. The exact calculation by numerical integration using equation (1) is also displayed in (*a*) (dashed line).

QB system. Again as the distance and the time increase, the resonance levels decay, first exponentially and then nonexponentially, as depicted in the inset of figure 3(*b*). Even at larger distances the decay is purely nonexponential, as an inverse cubic power of time, as shown by the inset in figure 3(*c*). Note that in figure 3(*c*) the profile of the transmitted wave packet already resembles the energy structure of the transmission coefficient.

It is of interest to compare our results with the case of a cutoff incident plane wave impinging on a multibarrier system. This case, corresponding to the limit of an infinitely broad Gaussian wave packet, has been considered recently by Villavicencio and Romo [43], using the formalism developed in [3], to investigate the propagation of transmitted quantum waves in these systems. There, for incidence energies E_0 below the lowest resonance energy of the multibarrier system, a series of propagating pulses (forerunners) are observed in the transmitted solution traveling faster than the main wavefront. It is shown that each forerunner propagates with speed $v(\mathcal{E}_n) = [2m\mathcal{E}_n/m]^{1/2}$ associated with the nth resonance of the system, thus establishing a relationship between the sequence of forerunners and the resonance spectrum

of the system. However, at asymptotically long times the forerunners fade away, since the solution $\psi(x,t) \sim \mathbf{t}(k_0)\exp(\mathrm{i}k_0x)\exp(-\mathrm{i}E_0t)/\hbar)$, with $k_0 = [2mE_0]^{1/2}/\hbar$. This yields for the transmitted probability density $|\psi(x,t)|^2 = |\mathbf{t}(k_0)|^2$, a result very different from the case of Gaussian wave packets of finite width considered here.

4.3. Reconstruction of the energy spectra

In order to exhibit more clearly the relationship between the time evolution of the transmitted Gaussian wave packet and the energy spectra of the system, pointed out in the previous subsection, one may proceed as follows. First, instead of evaluating the transmitted probability density by fixing $x = x_\mathrm{d}$ and varying the time t, i.e. $|\psi^\mathrm{a}(x_\mathrm{d},t)|^2$, as discussed in the previous subsection, we consider instead a fixed value of the time $t = t_0$ and vary x, i.e. $|\psi^\mathrm{a}(x,t_0)|^2$. It is not difficult to see that the plot of $|\psi^\mathrm{a}(x,t_0)|^2$ versus x looks identical to the specular image, with respect to the vertical axis at the origin, of $|\psi^\mathrm{a}(x_\mathrm{d},t)|^2$ versus t. Second, in analogy with the calculation of the transmission coefficient in the energy domain, we divide $|\psi^\mathrm{a}(x,t_0)|^2$ by the free evolving Gaussian wave packet $|\psi^\mathrm{a}_\mathrm{f}(x,t_0)|^2$, given by equation (16). We define the quantity $\zeta(x,t_0)$ as the ratio of these quantities, namely

$$\zeta(x,t_0) = \frac{|\psi^\mathrm{a}(x,t_0)|^2}{|\psi^\mathrm{a}_\mathrm{f}(x,t_0)|^2}. \tag{44}$$

Third, it is convenient to plot the transmission coefficient $T(E)$ in units of E/E_0, with E_0, the incident energy of the corresponding Gaussian wave packet. This allows us to relate the values of E/E_0 to the values of a parameter η defined as

$$\eta \equiv \left[\frac{x-L}{x_0-L}\right]^2. \tag{45}$$

The above expression for η is based on the argument that for $x \gg L$, $E = \hbar^2k^2/2m$ with $\hbar k/m = (x-L)/t_0$, and $E_0 = \hbar^2k_0^2/2m$ with $\hbar k_0/m = (x_0-L)/t_0$, where $x_0 - L$ is the distance that a free particle travels in time t_0. Hence, $E = \eta E_0$. Figure 4 exhibits, for the QB system, considered in the previous subsection, the plot of $\zeta(x,t_0)$ versus η. As indicated in the inset to the figure, each graph of $\zeta(x,t_0)$ corresponds to a distinct value of t_0 and hence of $x_0 - L$. The above figure also exhibits a plot of $T(E)$ in units of E/E_0 (solid line). One may appreciate, in each figure, the transient behavior of the transmitted Gaussian wave packet. For small values of t_0, $\zeta(x,t_0)$ reproduces the fastest components of the energy spectra of the system. As t_0 increases $\zeta(x,t_0)$ goes into a transient behavior that ends when the transmission energy spectra of the system is reconstructed, i.e. for $t_0 = 10^4\tau_\mathrm{QB}$ (dashed line), $\zeta(x,t_0)$ is already indistinguishable from $T(E)$, as shown analytically by equation (40).

5. Remark on the tunneling time problem

Our results are of relevance for the tunneling time problem [11]. Here, the question posed is: how long does it take for a particle to traverse a classical forbidden region? One of the approaches considered involves the tunneling of wave packets. Here one usually compares some feature of the incident free evolving wave packet (usually a Gaussian wave packet) and a comparable feature of the transmitted wave packet, commonly the peak or the centroid, and a delay is calculated. Many years ago, Büttiker and Landauer [45] argued that such a procedure seems to have little physical justification because an incoming peak or centroid does not, in any obvious causative sense, turn into an outgoing peak or centroid, particulary in the case of strong deformation of the transmitted wave packet. Our results for the transient behavior of

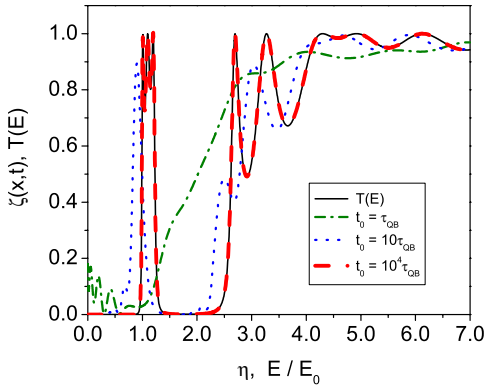

Figure 4. $T(E)$ stands for the transmission coefficient in units of E_0, the energy of the incident wave packet (solid line); $\zeta(x, t_0)$ defined by equation (44) in units of the parameter η, for distinct values of t_0, as specified in the insets to each figure. As time increases the transients end by reproducing the energy spectra of the QB system. See the text.

the transmitted wave packet support that view independently of whether or not there is initially a strong deformation of the transmitted wave packet. Even if the transmitted wave packet is not initially deformed, as time evolves the profile of the transmitted Gaussian wave packet varies to finally reproduce the energy spectra of the system and hence there is no unique way to answer the question of how long it took to the initial packet to traverse the system.

6. Concluding remarks

The main result of this work is given by equation (33), which provides an analytical solution to the time evolution of a Gaussian wave packet along the transmission region for scattering by a finite-range potential in one dimension. We have focused our investigation to cases where the Gaussian wave packet is initially far from the interaction region, i.e. fulfills equation (8), and is sufficiently broad in momentum space so that all sharp and broad resonances of the system are included in the dynamical description. We have obtained analytically and exemplified numerically for a multibarrier quantum system, using the resonant state formalism, that the transmitted Gaussian wave packet may be written as the product of the free evolving Gaussian wave packet and a transient term. We have shown that at very large distances and long times the transient term becomes proportional to the transmission amplitude of the system, i.e. equation (40). We have also obtained this last result by using the steepest descent method as follows from equation (42). It is also worth emphasizing that the analytical expression for the transmitted wave packet yields, at a fixed distance and asymptotically long times, a $t^{-3/2}$ behavior with time, i.e. equation (38). This result corroborates numerical calculations for Gaussian wave packets colliding with square barriers and extends previous analysis to arbitrary potentials of finite range [27]. One should recall that the set of poles $\{\kappa_n\}$ and residues $\{r_n\}$, which is unique for a given potential profile, is evaluated just once to calculate the time-dependent solution given by equation (33). The number of poles required for a dynamical calculation corresponds to the number of poles necessary to reproduce the exact transmission amplitude using equation (21). This is in contrast with calculations involving numerical integration of the solution, using equation (1), where one has to perform an integration over k at each instant of time and hence the calculation is much more demanding computationally

particularly at large distances and long times. Our analytical solution for the transmitted wave packet might be of interest in connection with the long-debated tunneling time problem. A final remark on extensions and ongoing work. The formalism discussed here may be extended in a straightforward way to discuss the time-dependent solution along the internal region of the potential in a similar fashion as considered for quasi-monochromatic waves [3]. This allows us to study the buildup of the quasistationary state formed in the scattering process. In order to study the subsequent time evolution of decay one needs to consider the reflection amplitude. This requires additional contributions to the corresponding resonance expansion that involve an extension of the formalism discussed here.

Acknowledgments

Would like to thank R Romo for discussions and the partial financial support of grants DGAPA-UNAM IN115108 and DGAPA-UNAM IN112410.

Appendix A. Analysis of $\omega(-\mathrm{i}z)$

Here we show that the contribution of the term $\omega(-\mathrm{i}z)$, appearing on the right-hand side of equation (7), to the time evolution of the transmitted Gaussian wave packet may be neglected provided the condition given by equation (8) is fulfilled. The contribution corresponding to $\omega(-\mathrm{i}z)$ reads

$$\psi_n^{\mathrm{ne}}(x,t) = -\frac{(2\pi)^{1/4}\sqrt{\sigma}}{\sqrt{\omega(\mathrm{i}z_0)}}\frac{1}{2\pi}\int_{-\infty}^{\infty}\mathrm{d}k\,\frac{\omega(-\mathrm{i}z)}{k-\kappa_n}\,\mathrm{e}^{\mathrm{i}kx-\mathrm{i}\hbar k^2 t/2m}, \tag{A.1}$$

where z, defined by equation (5), is written as $z = \mathrm{i}(k-k_0')\sigma$ with $k_0' = k_0 - \mathrm{i}x_c/2\sigma^2$. In general, it is necessary to calculate numerically the integral term given by equation (A.1). However, for the particular case specified by equation (8), i.e. $|x_c/2\sigma| \gg 1$, that implies that $|z| > 1$ for all values of k, one may use the asymptotic expansion of the Faddeyeva function $\omega(-\mathrm{i}z)$ [34, 35]:

$$\omega(-\mathrm{i}z) \approx -\frac{\mathrm{i}}{\pi}\sum_{j=0}^{N}\frac{\Gamma(j+1/2)}{[(k-k_0')\sigma]^{2j+1}}. \tag{A.2}$$

Since (A.2) is an asymptotic series it is sufficient to consider the leading term $j = 0$.

Substitution of equation (A.2) into equation (A.1) allows us to express the integral term in the sum as

$$\frac{\mathrm{i}}{2\pi}\int \mathrm{d}k\,\frac{\mathrm{e}^{\mathrm{i}kx-\mathrm{i}\hbar k^2 t/2m}}{(k-k_0')(k-\kappa_n)} = \frac{M(y_0')-M(y_n)}{k_0'-\kappa_n}, \tag{A.3}$$

where we have used the identity

$$\frac{1}{(k-k_0')(k-\kappa_n)} = \frac{1}{k_0'-\kappa_n}\left[\frac{1}{k-k_0'}-\frac{1}{k-\kappa_n}\right], \tag{A.4}$$

and the arguments of the Moshinsky functions $M(y_0')$ and $M(y_n)$ are given respectively by

$$y_0' = \mathrm{e}^{-\mathrm{i}\pi/4}\sqrt{\frac{m}{2\hbar t}}\left[x-\frac{\hbar k_0'}{m}t\right], \tag{A.5}$$

and

$$y_n = \mathrm{e}^{-\mathrm{i}\pi/4}\sqrt{\frac{m}{2\hbar t}}\left[x-\frac{\hbar \kappa_n}{m}t\right]. \tag{A.6}$$

Then, the nonexponential contribution of each pole κ_n in equation (A.1) reads

$$\psi_n^{\mathrm{ne}}(x,t) \approx \left(\frac{2}{\pi}\right)^{1/4} \frac{1}{\sqrt{\sigma}} \frac{M(y_0') - M(y_n)}{(k_0' - \kappa_n)\sqrt{\omega(\mathrm{i}z_0)}}. \tag{A.7}$$

Recalling that the factor $\sqrt{\omega(\mathrm{i}z_0)} = \exp\left(z_0^2/2\right)\sqrt{\mathrm{erfc}(z_0)}$ and that $z_0 \ll -1$ [34, 35] one obtains

$$\sqrt{\omega(\mathrm{i}z_0)} \approx \sqrt{2}\,\mathrm{e}^{x_c^2/4\sigma^2}. \tag{A.8}$$

It follows then, by the substitution of (A.8) into (A.7) and comparing the resulting expression with equation (29), taking into account that the corresponding Moshinsky functions yield contributions of the same order of magnitude, that

$$\left|\psi_n^{\mathrm{ne}}(x,t)\right| \sim \mathrm{e}^{-x_c^2/4\sigma^2}\left|\psi_n^{\mathrm{a}}(x,t)\right|. \tag{A.9}$$

The above expression demonstrates that provided equation (8) is satisfied, the nonexponential contribution ψ_n^{ne} may be neglected. For the example discussed in section 4, we obtain $\left|\psi_n^{\mathrm{ne}}(x,t)\right| \sim \mathrm{e}^{-25}\left|\psi_n^{\mathrm{a}}(x,t)\right|$, namely it yields a negligible contribution.

Appendix B. Calculation of complex poles of the transmission amplitude

It is well known that the transmission amplitude $\mathbf{t}(k)$ for a potential $V(x)$ of finite range, i.e. extending from $x = 0$ to $x = L$, possesses an infinite number of complex poles κ_n that in general are simple [37]. These complex poles correspond to the zeros of the element $t_{22}(k)$ of the corresponding transfer matrix

$$\mathbf{t}(k) = \frac{1}{t_{22}(k)}. \tag{B.1}$$

The set of complex poles of $\mathbf{t}(k)$ may be calculated using the Newton–Raphson method [39]. This method approximates a complex pole κ_n by using the iterative formula

$$\kappa_n^{r+1} \approx \kappa_n^r - \frac{t_{22}\left(\kappa_n^r\right)}{t_{22}'\left(\kappa_n^r\right)}, \tag{B.2}$$

where $t_{22}'(k) = \mathrm{d}t_{22}(k)/\mathrm{d}k$. The approximate pole κ_n^{r+1} goes into the exact pole, at a given degree of accuracy, as the number of iterations increases. In order to apply this method, it is necessary to provide an appropriate initial value for the approximate pole κ_n^0.

In general for systems formed by a few alternating barriers and wells, as exemplified by figure 2, the transmission coefficient versus energy may be roughly characterized by three regimes: regime I, characterized by sharp isolated resonances (as in figure 2(*b*)) or groups of well-defined overlapping resonances (as the resonance triplet in figure 2(*c*)). This regime occurs usually for energies below the potential barrier height and refers to complex poles that are seated close to the real k-axis; regime II, characterized by broad overlapping resonances. This regime is commonly found close to the potential barrier height and may extend up to energies three or four times the potential barrier height, as exemplified in all figures 2 and regime III, involving much higher energies, well above the barrier height. There the transmission coefficient does not exhibit any appreciable resonance structure and just fluctuates very closely around unity.

There is in general no analytical expression for any initial approximate pole κ_n^0. An exception occurs along regime III, where there exists an asymptotic formula for the location of complex poles which is valid for very large values of n [37]:

$$\kappa_n^0 \approx \frac{n\pi}{L} - \mathrm{i}\frac{2}{L}\ln(n) + O(1); \qquad n \gg 1. \tag{B.3}$$

One may substitute equation (B.3) into equation (B.2) to obtain the pole $\kappa_n = \alpha_n - \mathrm{i}\beta_n$ for that very large value of n, say for example, $n = 4000$. Equation (B.3) provides a relationship between the real parts of the $(n+1)$st and $(n-1)$st poles with the nth pole:

$$\alpha_{n\pm1} \approx \alpha_n \pm \frac{\pi}{L} \equiv a_{n\pm1}, \tag{B.4}$$

and for the corresponding imaginary parts

$$\beta_{n\pm1} \approx \beta_n. \tag{B.5}$$

Hence, one may write

$$\kappa^0_{n\pm1} \approx \kappa_n \pm \Delta_\mathrm{r}. \tag{B.6}$$

where the step Δ_r is given by

$$\Delta_\mathrm{r} = \frac{\pi}{L}. \tag{B.7}$$

Then, one may calculate the $(n-1)$st pole by substituting equation (B.6) into the iterative Newton–Raphson formula to evaluate the pole κ_{n-1}. Repeating this procedure successively allows us to generate the poles for smaller values of n. Clearly this procedure also permits us to obtain the poles for larger values of n. As the value of n diminishes, however, on may reach a situation where, even if n is still large, the iterative Newton–Raphson formula may fail. We have found that in this circumstance equation (B.7) still holds but equation (B.5) becomes inaccurate. In order to circumvent this situation one may proceed as follows. Once, as indicated above, it is determined that the pole κ_n is asymptotic and has been calculated, one defines a rectangular region I_{n-1} on the complex k plane whose center contains the pole κ^0_{n-1}. This region is characterized by

$$I_{n-1} = [a_{n-1} - \Delta_\mathrm{r}/2, a_{n-1} + \Delta_\mathrm{r}/2] \times [-\beta_n - \Delta_\mathrm{i}/2, -\beta_n + \Delta_\mathrm{i}/2], \tag{B.8}$$

where Δ_i is a controllable parameter. Since the imaginary values of neighboring poles do not differ substantially, it is sufficient to choose

$$\Delta_\mathrm{i} = \beta_n. \tag{B.9}$$

If, as indicated above, the iterative formula given by equation (B.2) fails for a given initial value κ^0_{n-1}, then a new initial value κ^0_{n-1} is generated randomly according to the expression

$$\kappa^0_{n-1} = \kappa_n - \Delta_\mathrm{r} + \gamma_\mathrm{r}\Delta_\mathrm{r} + \mathrm{i}\gamma_\mathrm{i}\Delta_\mathrm{i}, \tag{B.10}$$

where, the parameters γ_r and γ_i are random numbers that vary, respectively, along the intervals $-0.5 \leqslant \gamma_\mathrm{r} \leqslant 0.5$ and $-0.5 \leqslant \gamma_\mathrm{i} \leqslant 0.5$ to guarantee that the generated pole lies within the region I_{n-1}. If the condition $\left|t_{22}\left(\kappa^0_{n-1}\right)\right| < 1$ is fulfilled, then the iterative formula (B.2) is applied. Otherwise or if the calculated pole lies outside I_{n-1}, that pole is disregarded and a new initial pole is generated according to the above procedure. Usually, after a few random attempts convergence to a new pole is obtained. If after many random attempts ($M = 1000$ for the examples considered in this work) no convergence is achieved, that may suggest that regime II has been reached. This means that equation (B.7) does not hold anymore. Then, it is convenient to define from that pole inward thinner rectangular regions I_{n-1}. For the examples considered in this work, we choose $\Delta_\mathrm{r} = \pi/20L$ and for $\Delta_\mathrm{i} = 2\beta_n$. Clearly, in this case some rectangular regions do not possess any poles. This procedure is also capable to generate the poles in regime I. Although in regimes I and II the above procedure may generate repeated poles, a consequence that equation (B.4) does not hold, these poles may be easily identified and disregarded. For regime I there is the alternative simple procedure to generate the initial values κ^0_n by the rule of the half-width at half-maximum of the Breit–Wigner formula for the transmission coefficient.

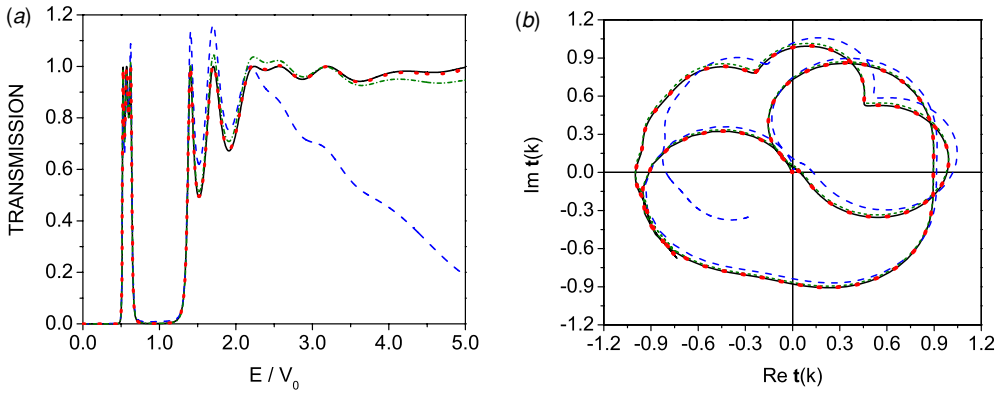

Figure B1. (*a*) Comparison of the transmission coefficient $T(E)$ as a function of energy in units of the potential height V_0 for the QB system of the exact calculation using the transfer matrix method (solid line) with resonance calculations using equation (21) for a number of poles: 10 (dashed line), 100 (dash-dot line) and 1000 (dotted line). (*b*) A similar calculation for the transmission amplitude Re$\mathbf{t}(k)$ versus Im$\mathbf{t}(k)$.

Once a set of N complex poles $\{\kappa_n\}$ has been obtained, one may evaluate the transmission amplitude given by equation (21), by running it from $-N$ to N. One might then make a comparison of the resonance expansion, for different values of the number of poles, with the exact numerical calculation using the transfer matrix method [1] to establish the appropriate number of poles for a given energy interval. Figure B1(*a*) provides a plot of the transmission coefficient *versus* energy for the QB system discussed in the text for the exact numerical calculation using the transfer matrix method (solid line) and resonance expansions of $\mathbf{t}(k)$ for distinct number of poles: $N = 10$ (dashed line), $N = 100$ (dash-dot line) and $N = 1000$ (dotted line). The energy interval extends up to five times above the barrier height and one sees that as the number of poles increases the agreement with the exact calculation becomes better. Note that already with $N = 100$ poles, the transmission coefficient is well reproduced for energies below the potential barrier height. Note also that the calculation involving 1000 poles is still slightly different from the exact calculation in the interval $4.0 < E/V_0 < 5.0$. The calculation for the same system presented in figure 20, that involved 4000 poles, is indistinguishable from the exact calculation. One sees that away from sharp resonances, more resonance terms are required to reproduce the exact calculation. This is particularly striking in energy intervals where $T(E)$ fluctuates very close to unity where a very large number of resonance terms is necessary to reproduce the exact calculation. Fortunately, very distant resonance poles are not difficult to calculate. Figure B1(*b*) exhibits similar calculations for the transmission amplitude. Here Re $\mathbf{t}(k)$ versus Im $\mathbf{t}(k)$ is plotted to show that the resonance expansions of the transmission amplitude become closer to the exact calculation as the number of poles in the calculation increases.

References

[1] Ferry D K and Goodnick S M 1997 *Transport in Nanostructures* (Cambridge: Cambridge University Press)
[2] Mizuta H and Tanoue T 1995 *The Physics and Applications of Resonant Tunnelling Diodes* (Cambridge: Cambridge University Press)
[3] García-Calderón G and Rubio A 1997 *Phys. Rev.* A **55** 3361
[4] Simanjuntak H P and Pereyra P 2003 *Phys. Rev.* B **67** 045301

[5] Konsek S L and Pearsall T P 2003 *Phys. Rev.* B **67** 045306
[6] Andreata M A and Dodonov V V 2004 *J. Phys. A: Math. Gen.* **37** 2423
[7] Fu Y and Willander M 2005 *J. Appl. Phys.* **97** 094311
[8] Granot E and Marchewka A 2005 *Europhys. Lett.* **72** 341
[9] Wulf U and Skalozub V V 2005 *Phys. Rev.* B **72** 165331
[10] MacColl L A 1932 *Phys. Rev.* **40** 621–6
[11] Landauer R and Martin T 1994 *Rev. Mod. Phys.* **66** 217
[12] Muga G, Mayato R S and Egusquiza I 2008 (ed) *Time in Quantum Mechanics* vol 1 (*Lecture Notes in Physics* no 734) (Berlin: Springer)
[13] García-Calderón G and Villavicencio J 2003 *Phys. Rev.* A **68** 052107
[14] Hartman T E 1962 *J. Appl. Phys.* **33** 3427
[15] Pérez A L, Brouard S and Muga J G 2003 *J. Phys. A: Math. Gen.* **36** 2371
[16] Bohm D 1989 *Quantum Theory* (New York: Dover)
[17] Muga J G, Egusquiza I L, Damborenea J A and Delgado F 2002 *Phys. Rev.* A **66** 042115
[18] Hernández A and García-Calderón G 2003 *Phys. Rev.* A **68** 014104
[19] Støvneng J A and Hauge E H 1991 *Phys. Rev.* B **44** 13582
[20] Harada N and Kuroda S 1986 *Jpn. J. Appl. Phys.* **25** L871
[21] Peisakhovich Y G and Shtygashev A A 2008 *Phys. Rev.* B **77** 075326
[22] Peisakhovich Y G and Shtygashev A A 2008 *Phys. Rev.* B **77** 075327
[23] Moshinsky M 1952 *Phys. Rev.* **88** 626
[24] Holland P R 1995 *The Quantum Theory of Motion* (Cambridge: Cambridge University Press)
[25] García-Calderón G, Villavicencio J and Yamada N 2003 *Phys. Rev.* A **67** 052106
[26] Villavicencio J, Romo R and Cruz E 2007 *Phys. Rev.* A **75** 012111
[27] Muga J G, Delgado V and Snider R F 1995 *Phys. Rev.* B **52** 16381
[28] Miyamoto M 2004 *Phys. Rev.* A **69** 042704
[29] García-Calderón G, Romo R and Villavicencio J 2007 *Phys. Rev.* B **76** 035340
[30] Torrontegui E, Muga J G, Martorell J and Sprung D W L 2009 *Phys. Rev.* A **80** 012703
[31] Anteneodo C, Dias J C and Mendes R S 2006 *Phys. Rev.* E **73** 051105
[32] del Campo A, García-Calderón G and Muga J 2009 *Phys. Rep.* **476** 1
[33] Brouard S and Muga J G 1996 *Phys. Rev.* A **54** 3055
[34] Faddeyeva V N and Terentev M N 1961 *Tables of Values of the Function* $\omega(z) = \mathrm{e}^{-z^2}(1 + \frac{2i}{\sqrt{\pi}} \int_0^z \mathrm{e}^{t^2} \mathrm{d}t)$, *for Complex Argument* ed V A Fock (London: Pergamon)
[35] Abramowitz M and Stegun I 1968 *Handbook of Mathematical Functions* (New York: Dover)
[36] García-Calderón G 1987 *Solid State Commun.* **62** 441
[37] Newton R G 2002 *Scattering Theory of Waves and Particles* 2nd edn (New York: Dover)
[38] Humblet J and Rosenfeld L 1961 *Nucl. Phys.* **26** 529
[39] Jüli E and Mayers D 2003 *An Introduction to Numerical Analysis* (Cambridge: Cambridge University Press)
[40] García-Calderón G, Romo R and Rubio A 1993 *Phys. Rev.* B **47** 9572
[41] Garcia-Calderon G and Peierls R 1976 *Nucl. Phys.* A **265** 443–60
[42] Poppe G P M and Wijers C M J 1990 *ACM Trans. Math. Softw.* **16** 38
[43] Villavicencio J and Romo R 2003 *Phys. Rev.* B **68** 153311
[44] Erdélyi A 1956 *Asymptotic Expansions* (New York: Dover)
[45] Büttiker M and Landauer R 1982 *Phys. Rev. Lett.* **49** 1739